

## Depth-dependent disordering in *a*-Si produced by self-ion-implantation

P. X. Zhang, I. V. Mitchell, B. Y. Tong, and P. J. Schultz

*Department of Physics, University of Western Ontario, London, Ontario, Canada N6A 3K7*

D. J. Lockwood

*Institute for Microstructural Sciences, National Research Council Canada, Ottawa, Canada K1A 0R6*

(Received 29 July 1994)

Raman scattering from amorphous silicon (*a*-Si) produced by self-ion-implantation reveals an exciting wavelength-dependent scattering-intensity ratio of the optical- and the acoustic-phonon-like peaks. The results show that this wavelength-dependent scattering originates from a depth-dependent disordering. The surface part ( $\sim 200$  Å) of the samples demonstrates weaker long-range disordering, while the internal part demonstrates stronger long-range disordering. After annealing at 500°C for an hour this inhomogeneity disappears. This is explained as the elimination of certain defects that strongly influence the longer-range order of the lattice. These defects relax spontaneously at the surface during the ion implantation.

There have been many papers devoted to the study of the properties of amorphous silicon (*a*-Si), due to the prominent applications of this material, as well as the basic physics behind it.<sup>1-5</sup> The most significant aspects of the material are the structural relaxation of, and the defects in, the continuous random network. Sinke *et al.*<sup>6</sup> studied the structural relaxation of *a*-Si using three different annealing processes and Raman spectroscopy. According to the position and linewidth of the transverse-optic (TO)-like phonon peak, they found that there are several relaxation processes, which occur on different time scales, and the relaxation is mainly related to the short-range disorder. Later, Roorda *et al.*,<sup>7</sup> using differential scanning calorimetry, showed that there is a one-time low-temperature heat release, which proved to be direct evidence for structural relaxation in *a*-Si. They also related this relaxation to the variation in the continuous random network of *a*-Si, and by reimplantation this relaxation state can be derelaxed.<sup>8</sup> Recent experiments have demonstrated the flexibility and the complexity of the ion-implantation technique in producing *a*-Si. According to the ion energy, dose, dose rate, the implantation temperature, and the type of substrate, the silicon can be damaged, amorphized, recrystallized, or form a buried layer.<sup>9,10</sup> Considerable efforts have been made to understand and to control these processes, as they strongly influence the electronic and structural as well as the thermodynamic properties of the *a*-Si. However, the properties of the *a*-Si produced by self-ion-implantation are still not very well characterized. One of the reasons for this is apparently due to the structural variations and inhomogeneity of *a*-Si, which are difficult to measure and characterize and hence were ignored for a long time. More recently, there have been discussions on the different defect structures in *a*-Si produced in the ion-implantation process.<sup>1,5</sup> Coffa and co-workers<sup>1</sup> have pointed out that according to the measured activation energy there are three types of defects in *a*-Si produced by ion implantation, while Stolk and co-workers<sup>5</sup> have

shown from the average bond-angle distortion  $\Delta\Theta$  derived from Raman spectroscopy that there is "another" defect, which contributes independently to the enthalpy of *a*-Si. These different defect identifications produce some information for understanding the ion-implantation process and the basic properties of *a*-Si. However, there are few reports on the structural information of these defects, although various methods of probing them have been used, such as *in situ* conductivity measurement,<sup>1</sup> photocarrier lifetime measurement,<sup>5</sup> Raman spectroscopy,<sup>1,5,10</sup> and differential scanning calorimetry.<sup>5</sup> Most of the measurements were conducted on the entire sample; there are not many methods that can be used to study details of the structure, especially depth profiling.

We report here the results of Raman scattering experiments in which several laser wavelengths were used. Due to their different absorption constants, these laser lines penetrate into different depths of the samples, and therefore a depth profiling was achieved. In addition, we paid special attention to the low-frequency acoustic-phonon-like Raman modes, which were often poorly measured previously, and now yield useful information. The Raman measurements on *a*-Si produced by self-ion-implantation reveal a laser wavelength-dependent scattering-intensity ratio of the optical- and acoustic-phonon-like peaks. Analysis shows that this originates probably from a depth-dependent structural inhomogeneity. It seems that the surface part of the samples is relatively weaker in long-range disordering, while the inner part is stronger. This depth-dependent structural inhomogeneity may originate from special defect structures, which relax easily at the surface but remain in the bulk. The behavior of this type of defect demonstrates some similarity to the defects mentioned by Stolk and co-workers.<sup>5</sup> This structural inhomogeneity will have an important influence on the analysis of the general electronic and thermodynamic properties of *a*-Si, especially since most studies so far have been performed on the bulk samples and the depth-dependent aspect has been neglected.

TABLE I. The laser wavelengths  $\lambda$  used and the corresponding absorption coefficients  $\alpha$  and their Raman penetration depths  $\delta$  in *a*-Si (Refs. 5,12, and 13).

$\lambda$ (nm)	457.9	488.0	514.5	568.2	647.1	676.4
$\alpha$ ( $10^5 \text{ cm}^{-1}$ )	6.0	4.8	3.5	1.8	1.0	0.75
$\delta$ (nm)	19.2	24.0	32.9	64.0	115.0	153.5

The amorphous sample was produced by 600-keV Si-ion-implantation in single-crystal (100) Si at liquid nitrogen temperature with a dose of  $10^{16}$  ion/cm<sup>2</sup> at a rate of  $5 \times 10^{12}$  ions/cm<sup>2</sup>/s. To avoid the channeling effect, the (100) surface of the silicon substrate was tilted 7° relative to the ion-beam direction. Further details of the implantation method are described elsewhere.<sup>10</sup>

The amorphous state of the surface layer of the silicon wafer was investigated by the Rutherford backscattering channeling (RBSC) technique, and its thickness was measured at the same time. The RBSC spectrum shows that the sample was amorphized right from the surface down and the thickness of the amorphous layer was 1330 nm. The Raman scattering measurements were performed at room temperature with a Spex 14018 Raman spectrometer. Due to the high optical absorption of the sample, a pseudobackscattering geometry was adopted.<sup>11</sup> Six laser wavelengths were used for the depth profiling: the 457.9, 488.0, 514.5, and 568.2, and 647.1 and 676.4 nm lines from Ar<sup>+</sup> and Kr<sup>+</sup> lasers, respectively. Precise optical-absorption coefficients  $\alpha$  are not available at these wavelengths for this ion-implanted sample. Hence we have to use the closest known values, which are listed in Table I,<sup>5,12,13</sup> together with the Raman penetration depth  $\delta$ . Raman signal intensities are an integration of all the scattered light from different depths,<sup>14</sup>

$$I(\omega) = I_0 \omega^4 \int_0^\infty \exp(-2\alpha z) \sigma_a dz, \quad (1)$$

where  $I_0$  is the incident light intensity,  $\sigma_a$  is the scattering efficiency of amorphous Si, which is supposed to be a constant,<sup>15</sup> and  $\omega$  is the laser frequency. Since the profiling is achieved by Raman measurements, we define the Raman penetration depth  $\delta$  as the distance  $z$  from the surface where the integrated scattered light intensity at the laser wavelength reached 90% of the total. The largest penetration depth is 153.5 nm at the 676.4-nm laser wavelength, which is still much smaller than the thickness (1330 nm) of the amorphous layer. Thus all of the scattered light is from *a*-Si and there is no contribution from the crystalline silicon substrate. The smallest penetration depth is 19.2 nm for the 457.9-nm laser wavelength, and all other laser wavelengths are probing depths in between 19.2–153.5 nm. Although this is a relatively shallow layer near the surface of the material, it provides a means of probing the homogeneity in this layer. The uncertainty in  $\alpha$  estimated from the results obtained by different authors<sup>5,12,13</sup> introduces some error into the calculated Raman penetration depths. However, the variation of nearly one order of magnitude in  $\alpha$  from 457.9 to 676.4 nm guarantees the validity of the depth profiling. Typical estimated error bars are indicated in the related figure.

Raman spectra are shown in Fig. 1(a) for selected laser

excitations. All these spectra demonstrate three typical Raman bands: the optical-phonon-like band located at  $\sim 470 \text{ cm}^{-1}$ , the acoustic-phonon-like band in the range 100–200  $\text{cm}^{-1}$ , and a mixed band in between. The spectra demonstrate that the surface layer of the sample is amorphized by the self-ion-implantation, as the typical 520  $\text{cm}^{-1}$  peak of crystalline silicon is not visible. A very pronounced variation in these spectra is the relative scattering intensities of the 470- and 100–200- $\text{cm}^{-1}$  bands. The 470- $\text{cm}^{-1}$  optical-phonon-scattering band originates from the destruction of the short-range order of the silicon lattice. We denote its intensity by  $I_o$ . The

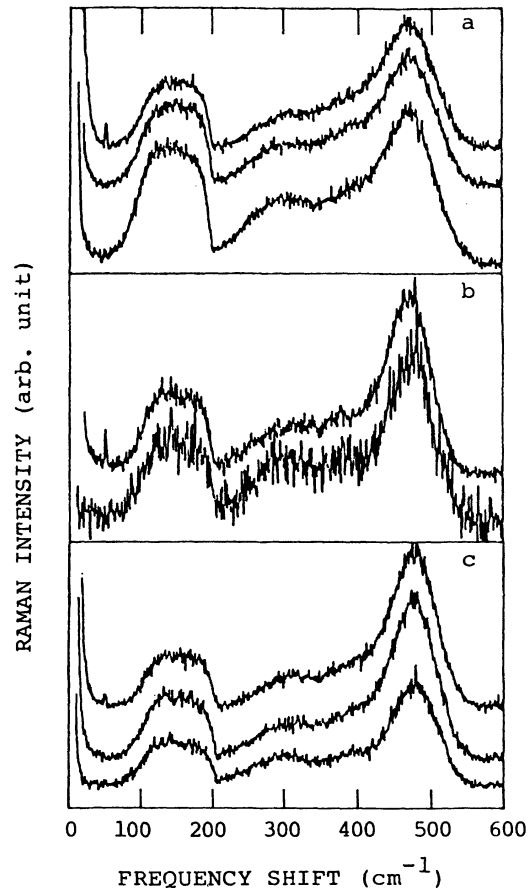


FIG. 1. (a) The Raman spectra of the *a*-Si sample produced by self-ion-implantation excited with 457.9- (upper trace), 514.5- (middle), and 647.1-nm (lower) laser lines (the base lines of the spectra are offset to illustrate the intensity variation clearly). (b) The Raman spectra of the *a*-Si sample produced by electron-beam evaporation excited with 457.9- (upper) and 647.1-nm (lower) laser lines. (c) The same as for (a) after annealing the sample at 500°C for 1 h. The sharp peak at 50  $\text{cm}^{-1}$  in the upper trace is an argon-laser plasma line.

TABLE II. The Raman scattering parameters of the self-ion-implanted *a*-Si sample obtained using different laser wavelengths and at room temperature (RT) and after annealing at 500°C: Raman shifts ( $\omega_o$ ) of the optical-phonon-like peaks, the linewidths of the optical- (acoustic-) phonon-like band  $\Delta\omega_o$  ( $\Delta\omega_a$ ), and the intensity ratio of the two bands  $\gamma = I_a/I_o$ .

Wavelength (nm)	$\omega_o$ (cm <sup>-1</sup> )		$\Delta\omega_o$ (cm <sup>-1</sup> )		$\Delta\omega_a$ (cm <sup>-1</sup> )		$\gamma = I_a/I_o$	
	RT	500°C	RT	500°C	RT	500°C	RT	500°C
457.9	470	475	40.8	36.5	95.3	96.1	0.52	0.35
488.0	470	475	40.1	33.1	96.9	98.0	0.59	0.37
514.5	470	475	42.5	35.8	98.7	96.6	0.62	0.39
568.2	470	476	41.9	34.4	98.0	96.4	0.71	0.45
647.1	470	477	39.7	34.4	103	98.4	0.76	0.44
676.4	472	480	39.5	35.1	102	100	0.80	0.43

100–200-cm<sup>-1</sup> band, which originates from the destruction of long- and/or intermediate-range order of the lattice, is a measure of the density of states of the acoustic phonons. We denote its intensity by  $I_a$ . Table II lists the measured parameters of the spectra, including the Raman shifts ( $\omega_o$ ) of the optical-like phonon, the optical- (and acoustic-) phonon-like band linewidths  $\Delta\omega_o$  ( $\Delta\omega_a$ ), and the intensity ratios  $\gamma = I_o/I_a$ . It can be seen for the as-implanted *a*-Si (in the column marked by RT in Table II) that  $\omega_o$  (470 cm<sup>-1</sup>) and  $\Delta\omega_o$  ( $\sim 35$  cm<sup>-1</sup>) of the optical-phonon-like peak show that the sample is in the so-called unrelaxed state and that the values obtained are in agreement with those measured by Sinke *et al.*<sup>6</sup> It is also clear that both  $\omega_o$  and  $\Delta\omega_o$  show no noticeable laser wavelength dependence. Only the intensity ratio  $\gamma$  shows such a dependence, and the shorter the laser wavelength the smaller the intensity ratio.

There are two possible mechanisms that may account for the observed laser-wavelength-dependent scattering. As the absorption coefficients are different and hence the penetration depths of these laser lines are different, the variation of the scattering parameters such as the intensity ratio  $\gamma$  may reflect directly the depth-dependent structural inhomogeneity of *a*-Si. The other possibility is resonant Raman scattering. It is well known<sup>16</sup> that when either the incident or the scattered light wavelengths approach an energy level of the material, resonance scattering will occur. In this process, the Raman intensity of those modes that are strongly coupled with the transition to the related energy level will be resonantly enhanced. In semiconductor materials, the acoustic- and optical-phonon-like modes may couple differently with some energy level, and hence the scattering behavior can be different.

To differentiate between these two possibilities, we conducted a reference experiment. A homogeneous *a*-Si layer produced by electron-beam evaporation<sup>17</sup> was measured at these same laser wavelengths. It is known that the physical properties of an evaporated film can differ by many orders of magnitude depending on the production parameters. The film we used here is in the so-called stable state of *a*-Si.<sup>18</sup> Figure 1(b) shows the results from the 457.9- and 647.1-nm laser wavelengths. It is clear that the two curves show the same intensity ratio ( $\sim 0.46$ ) for the optical and acoustic-phonon-like bands. This demonstrates that the resonance scattering, if there

is any, does not influence the relative intensities in this sample, and that the *a*-Si sample formed by electron-beam evaporation is homogeneous in the probed region. The ion-implanted sample may be different from the electron-beam evaporated one, and thus the possibility of some resonance effect can not be absolutely ruled out. However, an investigation of the measured optical absorption of amorphous silicon shows that the absorption edge is far from the wavelengths used for the Raman experiments.<sup>5,12,22</sup> Hence a resonance effect is not likely to occur in this sample. Thus we believe that this laser wavelength-dependent variation in the scattering parameters is largely due to the structural inhomogeneity of the materials.

The inhomogeneity is not induced by laser heating during the Raman experiments. We proved this by an experiment in which laser powers of 30 and 300 mW at 457.9 nm were used. If there is a laser heating effect the one from 457.9 nm would be the strongest, since the absorption coefficient at this wavelength is the largest of all the laser wavelengths. The Raman results showed no difference between the two recorded spectra, except for the longer measurement time needed to obtain the same scattering intensity for the 30-mW incident beam compared to the 300-mW one.

Raman signals arise from the lattice vibrations in solids and relate directly to the microstructure of the material. Raman spectra of both crystalline and amorphous silicon have been discussed extensively.<sup>10,19,20</sup> It has been concluded that the optical-phonon-like band in *a*-Si reflects the density of states of the optical phonons. The optical phonons are primarily related to the bonding between nearest-neighbor atoms, i.e., to short-range order, while the acoustic-phonon scattering is related more to the intermediate or long-range order. Hence the relative intensity of the two Raman bands may be taken as a measure of the weight of the short- to long-range order (or disorder in amorphous materials). Figure 2 shows the results of the measured intensity ratios at different laser wavelengths. According to the above argument that different laser wavelengths probe different depths of the sample, the curve then can be transferred to a depth dependency. Based on the measurements, it is clear that the variation of the scattering intensity ratio is largest on the surface part of sample and smallest inside. It seems that there is an approach to saturation from the surface towards the

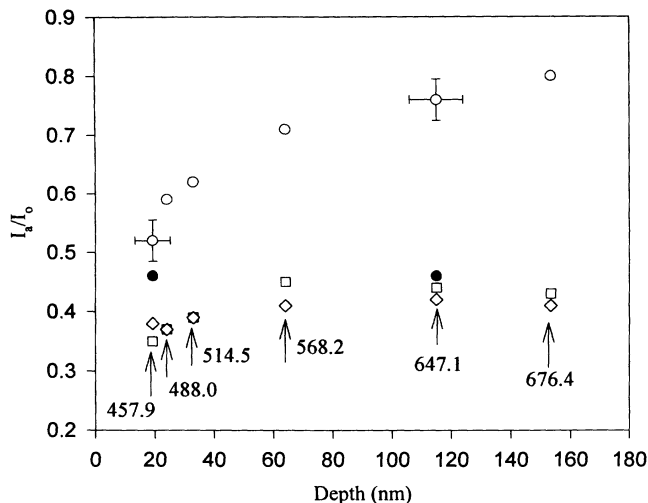


FIG. 2. The Raman intensity ratio of the acoustic- and optical-phonon-like scattering for the self-ion-implanted sample as a function of the excitation laser wavelengths, indicated by the arrows and the numbers (in nm), and the corresponding Raman penetration depth:  $\circ$ , as-implanted, and  $\diamond$  and  $\square$  after annealing at 500 and 550 °C, respectively. The estimated error due to the inaccuracy of the absorption constants and the measured scattering intensities ( $I_o, I_a$ ) are shown by the error bars for 457.9- and 647.1-nm wavelengths. The full circles show the intensity ratio obtained from the electron-beam evaporated sample at 457.9 and 647.1 nm, respectively.

interior of the sample. Such a variation provides a hint to understanding the results. The profile of the measured  $I_o/I_a$  is a response to a certain distribution of defects. The number of defects is very small at the surface and increases gradually towards the interior and finally reaches the saturation value of the bulk. Considering the ion-implantation process, there are various types of defects that may be produced and annihilated during the implantation. We suppose that some of the defects may easily diffuse to the surface and be annihilated there at an elevated temperature due to the irradiation<sup>21</sup> or at just room temperature, while inside the sample many of these defects remain due to a limited diffusion length. Hence a distribution profile of the defects was formed during the implantation and this has been reproduced by the Raman intensity ratio.

If this explanation is true then the distribution should disappear upon eliminating the defects by, for example, annealing. There are several reports<sup>5,6</sup> that indicate that annealing at 500 °C for 1 h produces structural relaxation and defect annihilation. Parts of the self-ion-implanted sample were annealed in a nitrogen atmosphere for 1 h at 500 and 550 °C, respectively, and after each annealing the sample was measured again by the different laser wavelengths. The results are shown in Fig. 1(c), and the evaluated intensity ratios  $\gamma$  are shown in Fig. 2 by the  $\diamond$  (500 °C) and  $\square$  (550 °C) symbols. The scattering parameters obtained after annealing are also listed in Table II.

It is apparent that there are two types of variations.

The acoustic-phonon-like peak was much reduced in relative intensity upon annealing, and accordingly the corresponding defects were largely annihilated in the process. The variation of  $\gamma$  with depth is much reduced or has disappeared, and it approaches a value corresponding to that of the surface. The sample has become rather homogeneous. The second type of variation is demonstrated in the peak position shift and the linewidth narrowing of the optical-phonon peak, which shows that upon annealing the *a*-Si reaches the so-called relaxed state at the same time. The average bond-angle distortion is reduced from 11° to 9°, according to the analysis given in Ref. 19. The Raman frequency shift and linewidth narrowing do not show a depth dependence. This means that the short-range disorder is not depth sensitive either before or after the annealing. These variations, which follow the state change from the as-implanted *a*-Si to a relaxed one, are not directly related to the variation of the intensity ratio  $\gamma$ . The two types of variation upon annealing support the *a*-Si model<sup>5</sup> in which the amorphous silicon produced by ion implantation is described by a continuous random network and distributed defects. The defects, characterized by the low-frequency acoustic-phonon-like scattering peak, show several similarities in behavior with the defects described by Stolk and co-workers.<sup>5</sup> Using photocarrier lifetime measurements and Raman spectroscopy, they investigated the correlation between defect annihilation and bond-angle relaxation in *a*-Si. They showed that the defect population produced by ion implantation in both *c*-Si and relaxed *a*-Si are similar, and also that these defects were annihilated at about 500 °C. In our case, the defects appear upon ion implantation in crystalline silicon and also in the amorphous silicon sample. We have argued<sup>10</sup> that these defects affect the intensity of the low-frequency Raman band (100–200  $\text{cm}^{-1}$ ). In addition, the annealing temperature we used to reduce the number of the defects happens to be the same as theirs. It is noteworthy that annealing at 500 °C causes both network relaxation and annihilation of the defects.

In conclusion, we have probed the surface layer of self-ion-implanted Si by the Raman scattering technique, and a laser-wavelength-dependent scattering-intensity ratio for the acoustic- and optic-phonon-like modes was discovered. This dependence was determined to be due to a depth-related effect, since the different laser lines penetrate into different depths of the sample. Hence a structural inhomogeneity was revealed, which was not observed in an *a*-Si sample produced by electron-beam evaporation. This inhomogeneity seems to originate from the surface relaxation of certain defects during the implantation process. These defects are related to some extent to the acoustic-phonon-like scattering, and have a strong influence on the long- and/or intermediate-range disorder. They can be removed by annealing at 500 °C for  $\sim 1$  h and show a similarity to the defects discovered in the photocarrier lifetime measurements of Stolk and co-workers.

The authors would like to thank R. D. Goldberg for

providing samples and H. J. Labbé and M. Davis of NRC for experimental assistance in the Raman measurements and in annealing the sample, respectively. Research conducted in the UWO Tandetron Laboratory is supported

by grants from the Natural Sciences and Engineering Research Council of Canada, and by the Ontario Centre for Materials Research. P. Zhang thanks the CCP at the University of Western Ontario for financial support.

- <sup>1</sup>S. Coffa, F. Priolo, and A. Battaglia, *Phys. Rev. Lett.* **70**, 3756 (1993).
- <sup>2</sup>S. Roorda, W. C. Sinke, J. M. Poate, D. C. Jacobson, S. Dierker, S. B. Dennis, D. J. Eaglesham, F. Spaepen, and P. Fuoss, *Phys. Rev. B* **44**, 3702 (1991).
- <sup>3</sup>N. Hayashi, R. Suzuki, M. Hasegawa, N. Kobayashi, S. Tanigawa, and T. Mikado, *Phys. Rev. Lett.* **70**, 45 (1993).
- <sup>4</sup>P. J. Simpson, M. Vos, I. V. Mitchell, C. Wu, and P. J. Schultz, *Phys. Rev. B* **44**, 12 180 (1991).
- <sup>5</sup>P. A. Stolk, Ph.D. thesis, Universiteit Utrecht, The Netherlands, 1993.
- <sup>6</sup>W. Sinke, T. Warabisako, M. Miyao, T. Tokuyama, S. Roorda, and F. W. Saris, *J. Non-Cryst. Solids* **99**, 308 (1988).
- <sup>7</sup>S. Roorda, S. Doorn, W. C. Sinke, P. M. L. O. Scholte, and E. van Loenen, *Phys. Rev. Lett.* **62**, 1880 (1989).
- <sup>8</sup>S. Roorda, J. M. Poate, D. C. Jacobson, B. S. Dennis, S. Dierker, and W. C. Sinke, *Appl. Phys. Lett.* **56**, 2097 (1990).
- <sup>9</sup>S. Coffa, A. Battaglia, and F. Priolo, in *Materials Synthesis and Processing using Ion Beams*, edited by R. J. Culbertson, O. W. Holland, K. S. Jones, and K. Maex, MRS Symposia Proceedings No. 316 (Materials Research Society, Pittsburgh, 1994), p. 3.
- <sup>10</sup>P. X. Zhang, R. D. Goldberg, I. V. Mitchell, P. J. Schultz, and D. J. Lockwood, in *Materials Synthesis and Processing using Ion Beams* (Ref. 9), p. 87.
- <sup>11</sup>P. X. Zhang, D. J. Lockwood, H. J. Labbé, and J.-M. Baribeau, *Phys. Rev. B* **46**, 9881 (1992).
- <sup>12</sup>L. Ley, in *Hydrogenated Amorphous Silicon II*, edited by J. D. Joannopoulos and G. Lucovsky (Springer-Verlag, Berlin, 1984), p. 140.
- <sup>13</sup>J. Humlicek, M. Garriga, M. I. Alonso, and M. Cardona, *J. Appl. Phys.* **65**, 827 (1989).
- <sup>14</sup>See, for example, *Light Scattering in Solids*, edited by M. Cardona and G. Guntherodt (Springer-Verlag, Heidelberg, 1975), p. 25.
- <sup>15</sup>The scattering efficiency  $\sigma_a$  may vary due to the inhomogeneity of the  $\alpha$ -Si, although the variation must be small. Since precise data are not available, we take it as a constant.
- <sup>16</sup>See, for example, *Light Scattering in Solids (II)*, edited by M. Cardona and G. Guntherodt (Springer-Verlag, Heidelberg, 1984), p. 22.
- <sup>17</sup>G. Yang, P. Bai, Y.-J. Wu, B. Y. Tong, S. K. Wong, J. Du, and I. Hill, in *Materials Issues in Microcrystalline Semiconductors*, edited by P. M. Faucher, K. Tanaka, and C. C. Tsai, MRS Symposia Proceedings No. 164 (Materials Research Society, Pittsburgh, 1990), p. 321.
- <sup>18</sup>P. K. John, B. Y. Tong, and S. K. Wong, U.S. Patent No. 4402762 (1983).
- <sup>19</sup>R. Tsu, J. G. Hernandez, and F. H. Pollak, *Solid State Commun.* **54**, 447 (1985).
- <sup>20</sup>L. P. Avakyantz and E. D. Obratsova, in *Proceedings of 13th International Conference on Raman Spectroscopy*, edited by W. Kiefer *et al.* (Wiley, New York, 1992), p. 985.
- <sup>21</sup>A. Wittkower and J. K. Hirvonen, *Nucl. Instrum. Methods Phys. Rev. B* **6**, 78 (1985).
- <sup>22</sup>M. Fried, T. Lohner, W. A. M. Aarnink, L. J. Hanekamp, and A. van Silfhout, *J. Appl. Phys.* **71**, 5260 (1992).